Mamm Genome (2010) 21:350–360
DOI 10.1007/s00335-010-9272-8

Mitochondrial retention of Opa1 is required for mouse embryogenesis

Billie A. Moore · Gladys D. Gonzalez Aviles · Christine E. Larkins · Michael J. Hillman · Tamara Caspary

Received: 5 March 2010 / Accepted: 21 June 2010 / Published online: 21 July 2010

Abstract Mitochondria are dynamic cellular organelles that balance fission and fusion to regulate organelle morphology, distribution, and activity, and Opa1 is one of three GTPases known to regulate mitochondrial fusion. In humans, loss of a single Opa1 allele causes dominant optic atrophy, a degenerative condition that leads to loss of vision. Here we demonstrate that the *lilR3* mutant mouse phenotype is due to a point mutation in the *Opa1* gene resulting in mislocalized Opa1 protein from the mitochondria to the cytosol. Importantly, the mutation is in the middle domain of the Opa1 protein, for which no function had been described. Lack of mitochondrial retention of Opa1 is sufficient to cause the cellular Opa1 loss-of-function phenotype as the mitochondria are fragmented, indicating an inability to fuse. Despite the normally ubiquitous expression of Opa1 and the essential nature of mitochondria, embryos with aberrant Opa1 survived through midgestation and died at E11.5. These mutants displayed growth retardation, exencephaly, and abnormal patterning along the anterior-posterior axis, although the A–P axis itself was intact. The complex relationship between mitochondrial dynamics and cell death is emphasized by apoptosis in specific cell populations of *lilR3* embryos. Our results define, for the first time, a function of the middle domain of the Opa1 protein and demonstrate that mitochondrial retention of Opa1 protein is essential for normal embryogenesis.

B. A. Moore · G. D. Gonzalez Aviles · C. E. Larkins · M. J. Hillman · T. Caspary (✉)
Department of Human Genetics, Emory University School of Medicine, 615 Michael St., Suite 301, Atlanta, GA 30322-1047, USA
e-mail: tcaspar@emory.edu

C. E. Larkins
Graduate Program in Biochemistry, Cell and Developmental Biology, Emory University, Atlanta, GA 30322, USA

Present Address:
M. J. Hillman
Atlanta Research and Education Foundation, Decatur, GA 30033, USA

M. J. Hillman
Centers for Disease Control and Prevention, Atlanta, GA 30333, USA

M. J. Hillman
Veterans Affairs Medical Center, Atlanta, GA 30033, USA

Introduction

Eukaryotic cells regulate mitochondrial shape and function through the complementary processes of mitochondrial fission and fusion. Normal fission and fusion protect mitochondria from becoming isolated, autonomous organelles that would be susceptible to depletion of substrates and metabolites or mutations in the mitochondrial DNA (mtDNA). When these dynamics are lacking, mitochondria develop abnormal morphologies (reviewed in Detmer and Chan 2007). The biological significance of these dynamics is clear, since disrupting them leads to alterations in apoptosis, calcium buffering, and ATP production (Duchen 2000; Kroemer and Reed 2000; Rizzuto et al. 2000). Mutations in a number of genes that regulate mitochondrial dynamics have been associated with several human neurodegenerative diseases (reviewed in Chen and Chan 2009; Knott et al. 2008). Furthermore, neurons are found to be especially susceptible to disruptions in fission and fusion, although it remains unclear why this is so given the fundamental role of mitochondria in all cells.

The core proteins regulating fission and fusion are well known. Fission is regulated by two GTPases: dynamin-related protein 1 (Drp1) and fission 1 (Fis1) (Bleazard et al. 1999; Fekkes et al. 2000; James et al. 2003; Labrousse et al. 1999; Mozdy et al. 2000; Smirnova et al. 2001; Tieu and Nunnari 2000; Yoon et al. 2003). Fusion is mediated by the mitochondrial outer-membrane proteins mitofusin 1 and 2 (Mfn1 and Mfn2), as well as the mitochondrial inner-membrane protein Opa1 (Chen and Chan 2004; Hales and Fuller 1997; Hermann et al. 1998; Rapaport et al. 1998). Mitochondria lacking the Mfns or Opa1 are unable to fuse and therefore appear fragmented, whereas loss of either Drp1 or Fis1 causes mitochondria to elongate and form long, continuous tubules (Chen et al. 2005; Cipolat et al. 2004; Griparic et al. 2004; Lee et al. 2004; Smirnova et al. 2001).

Opa1 is a dynamin family GTPase containing two coiled-coil domains, a mitochondrial import sequence, the GTPase domain, and an uncharacterized region called the middle domain. Opa1 is known to function independently in mitochondrial fusion and cellular apoptosis (Frezza et al. 2006; Spinazzi et al. 2008). There are eight isoforms of Opa1 that exist due to alternative splicing of exons 4, 4b, and 5b (Delettre et al. 2001; Olichon et al. 2007; Song et al. 2007). Exon 4 mediates the fusion of the mitochondrial network, whereas exons 4b and 5b are essential in the release of cytochrome *c,* an apoptotic response. In addition, Opa1 post-translational processing cleaves the protein into long and short isoforms that oligomerize to mediate fusion (Delettre et al. 2001; Griparic et al. 2007; Herlan et al. 2003; Merkwirth et al. 2008; Park et al. 2005; Song et al. 2007).

Opa1 has been well studied as the gene most frequently mutated in autosomal dominant optic atrophy (ADOA), one of the most common forms of inherited blindness affecting 1 in 12,000-50,000 individuals (Alexander et al. 2000; Delettre et al. 2000; Kivlin et al. 1983; Kjer et al. 1996). While the cause of ADOA is widely accepted as haploinsufficiency, the reason for the specific sensitivity of the retinal ganglion cells remains unclear. In an effort to develop animal models for ADOA, two groups have examined the heterozygous mouse phenotype associated with distinct point mutations in *Opa1* (Alavi et al. 2007; Davies et al. 2007). In both alleles, they found less Opa1 in protein extracts from heterozygous mutants than in extracts from wild-type controls, supporting the notion that haploinsufficiency underlies ADOA. Furthermore, the animal models showed progressive phenotypes in the eye that paralleled the human disease. In the course of these analyses, the groups reported that mice homozygous for either Opa1 mutation are embryonic lethal, since there were no homozygous mutant pups resulting from heterozygous intercrosses; however, in neither case did they specifically characterize the phenotype (Alavi et al. 2007; Davies et al. 2007).

Here we identify and provide the first molecular characterization of the embryonic phenotype of a novel ENU-induced *Opa1* mouse mutation, *lilR3*. *lilR3* mutant embryos die at E11.5 due to loss of mitochondrial retention of Opa1. The *lilR3* mutation disrupts a conserved amino acid in an uncharacterized domain of the protein, indicating that this domain is required for Opa1 localization to mitochondria. Embryos with mislocalized Opa1 specify the basic body plan normally; however, as the embryos begin the growth and differentiation phase of embryogenesis, they die. We find abnormal signaling in pathways known to be necessary for the differentiation of specific cell fates in the posterior of the embryo. Surprisingly, the same pathways are normal in the anterior of the embryo, where we see increased cell death. These results indicate that the lack of Opa1 affects different cell types in distinct ways, reminiscent of the human disease state in which specific neural cells are most sensitive to Opa1 dosage.

Results

Meiotic mapping and sequencing identify *Opa1* mutation in *lilR3*

In the course of a chemical mutagenesis screen for recessive mutations critical in mammalian embryogenesis, we found the *lilR3* mutant line as a result of its small size, failure to properly rotate along the axis, and exencephaly at E9.5 (Garcia-Garcia et al. 2005). As we induced the *lilR3* mutation on a C57BL/6 background, we performed a backcross to C3H/HeJ to map and identify the mutation by sequencing candidate genes (see Experimental Procedures for details). From this sequencing we identified a single mutation: an A → G transition mutation in intron 19 of *Opa1* that created a cryptic splice acceptor site (Fig. 1). From the sequencing of *Opa1* cDNA extracted from *lilR3* embryos, we verified that the predominant transcript produced from the mutant allele used the cryptic splice site, resulting in a 6-bp insertion of intronic sequence. This aberrant transcript was predicted to result in the translation of a cysteine (C) in place of a tryptophan (W) at amino acid 616, as well as the addition of amino acids leucine (L) and arginine (R) due to the translation of intronic sequence (W616CinsLR). These amino acids lie within the middle domain, a highly conserved but uncharacterized domain of the Opa1 protein. The disrupted tryptophan residue is an invariant amino acid in Opa1 homologs in flies, worm, and human. Furthermore, there are three ADOA patients whose mutations disrupt W616 in Opa1 (Alexander et al. 2000; Ferre et al. 2009).

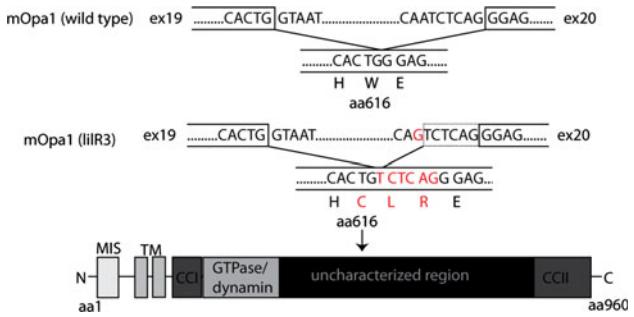

Fig. 1 The putative causative mutation of *lilR3* is located in *Opa1*. Illustration of wild-type and *Opa1*^{lilR3} sequences of the mutated region. An A → G transition in intron 19 creates a cryptic splice site that results in the insertion of six intronic bases in frame with the Opa1 coding sequence. A new codon results from the use of the cryptic splice acceptor between exons 19 and 20. This results in a C in place of a W at amino acid 616. The addition of the intronic sequences creates codons for L and R. These mutated amino acids are within an uncharacterized domain of the Opa1 protein called the middle domain

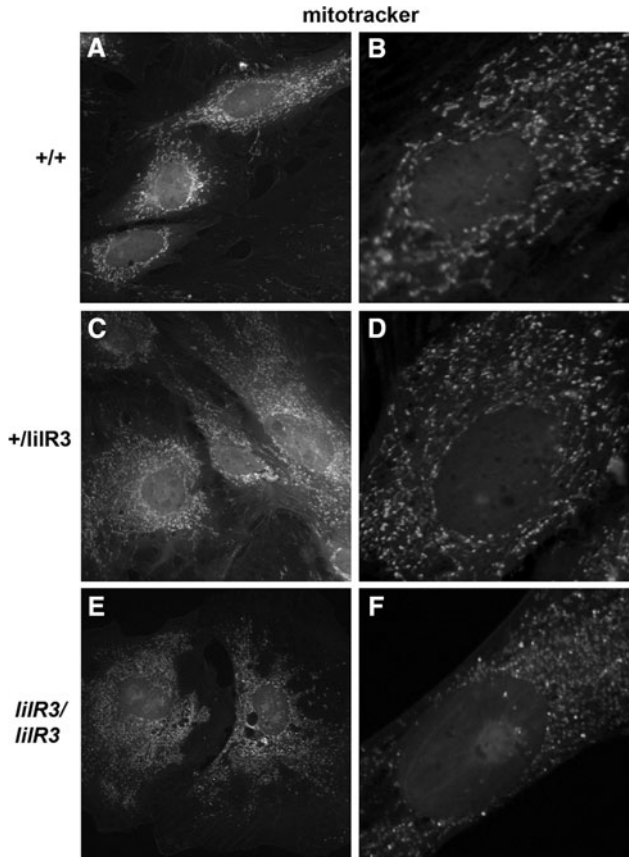

Fig. 2 The *lilR3* mutation leads to mitochondrial fragmentation. Using MitoTracker dye to visualize the mitochondria in primary mouse embryonic fibroblasts (MEFs). **a**, **b** Wild-type MEFs display an abundance of tubular mitochondrial networks in their cytoplasm, with only a small population of the mitochondria being fragmented. **c**, **d** Heterozygotes for the *lilR3* mutation show a mixture of fragmented and tubular mitochondria. **e**, **f** Homozygous *lilR3* mutant MEFs display mostly fragmented mitochondria in their cytoplasm

Opa1 is one of three GTPases known to regulate mitochondrial fusion. When Opa1 is knocked down in cells, mitochondrial fragmentation results (Chen et al. 2005; Cipolat et al. 2004; Griparic et al. 2004; Olichon et al. 2003). To determine whether the mutation we found in *Opa1* disrupts Opa1 function, we examined mitochondrial morphology in vivo. To circumvent technical difficulties associated with doing this in whole embryos, we isolated primary mouse embryonic fibroblasts (MEFs) from E10.5 embryos and used MitoTracker to visualize the morphology of the mitochondria using confocal microscopy (Fig. 2). In the wild-type MEFs, we saw morphologically normal mitochondria. However, in *lilR3* heterozygous and homozygous MEFs, we observed fragmentation of the mitochondria consistent with the *lilR3* mutation disrupting Opa1 function. The importance of Opa1 dosage was underscored by a more severe fragmentation phenotype in the homozygous mutant MEFs.

The dosage effect and fragmentation phenotype of the *lilR3* mutation suggested that it is a loss-of-function mutation. To investigate this we performed Western blot analysis on protein extracts from wild-type, heterozygous, and *lilR3* mutant E10.5 embryos using an antibody that recognizes the C-terminus of the Opa1 protein, a domain common to all isoforms (Misaka et al. 2002) (Fig. 3). As Opa1 localizes to the inner mitochondrial membrane, we separated the mitochondrial protein fraction from the cytosolic cellular fraction by centrifugation. As expected, in wild-type embryos we found Opa1 protein predominantly in the mitochondrial fraction, which was confirmed by the presence of cytochrome *c*. In heterozygous protein extracts we saw Opa1 protein in both the cytosolic and mitochondrial fractions, suggesting that the *lilR3* mutation caused Opa1 to mislocalize from the mitochondria. This was confirmed in our analysis of the homozygous fractions where we observed all Opa1 protein in the cytosolic fraction. We confirmed that we were analyzing equivalent amounts of total protein in all lanes by reprobing the blot with antibody against tubulin. Thus, Opa1 protein containing the W616CinsLR mutation results in stable mislocalized protein.

Morphological defects of the *Opa1*^{lilR3} homozygous mutant

We identified *Opa1*^{lilR3} due to its obvious morphological defects at E9.5: developmental delay, failure to properly rotate the body along the axis, small size, and exencephaly (Fig. 4a–d). At E8.5, *Opa1*^{lilR3} heterozygous and homozygous mutant embryos are indistinguishable from their wild-type littermates. By E10.5, *Opa1*^{lilR3} homozygous mutants

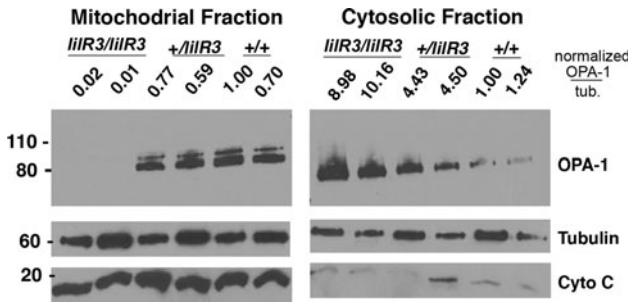

Fig. 3 Mislocalization of Opa1 protein in *lilR3* embryos. Western blot analysis of mitochondrial (*left panels*) and cytosolic (*right panels*) E10.5 embryo protein lysates using antibodies against Opa1, α-tubulin (loading control), and cytochrome *c* (mitochondrial marker, demonstrating the efficiency of fractionation). Normalized Opa1 expression is designated for each lane as the ratio of Opa1/tubulin expression relative to a wild-type sample set to 1. Opa1 is enriched in the wild-type (+/+) mitochondrial fraction, consistent with its known localization to the mitochondrial inner membrane. Opa1 is present in both the mitochondrial and cytosolic fractions from heterozygous (+/*lilR3*) extracts, whereas Opa1 is exclusively in the cytosolic fraction from homozygous (*lilR3/lilR3*) mutant extracts, indicating that the *lilR3* mutation causes Opa1 to mislocalize from the mitochondria. Upon overexposure, a faint band of Opa1 is visible in the mitochondrial fraction of the homozygous mutant extract (data not shown). Thus, the W616CinsLR mutation in the Opa1 middle domain disrupts the mitochondrial localization of Opa1, consistent with the *lilR3* allele being a strong loss-of-function mutation

appeared to have grown but were still much smaller than littermate controls. Craniofacial defects, including hypomorphic arches and clefting of the nasal process, were apparent (Fig. 4a, b upper inset). We also found hemorrhaging, indicating defects in vascular integrity (Fig. 4c, d). The $Opa1^{lilR3}$ somites were smaller and seemed disorganized compared with the solid cube structures of the littermate controls (Fig. 4a, b lower inset). At E11.5, the hearts stopped beating indicating the time of lethality in the $Opa1^{lilR3}$ embryos. The fact that the $Opa1^{lilR3}$ homozygous mutants displayed overall developmental and growth delay reflects the ubiquitous expression of Opa1 (Rochais et al. 2009).

Key signaling pathways in embryonic development are disrupted in the $Opa1^{lilR3}$ homozygous mutant

Considering the morphological defects of the $Opa1^{lilR3}$ embryos, we examined genes known to regulate the development of the disrupted tissues. For example, hypomorphic pharyngeal arches and vascular defects can be the result of improper neural crest development. Some of the pathways important in neural crest development also regulate neural tube closure, as well as somitogenesis, all of which are disrupted in $Opa1^{lilR3}$. Therefore, we examined the expression of several genes that are required markers of these important processes: *Sox10*, *Pax3*, *Wnt1*, and *Msx1*.

Sox10 is a transcription factor required for proper neural crest development. It maintains early-stage multipotency and directs late-stage non-neuronal fates in neural crest cells (Kim et al. 2003). In mice, *Sox10* is expressed in pre- and post-migratory neural crest cells all along the A–P axis. By E9.5, the neural crest has almost completed its emigration from the dorsal neural tube to ventral target tissues. We saw *Sox10*-positive neural crest in the pharyngeal region migratory streams and along the dorsal neural tube in both the control and $Opa1^{lilR3}$ mutant E9.5 embryos (Fig. 5a, b). However, the posterior boundary of *Sox10* expression is further anterior in the $Opa1^{lilR3}$ mutant embryos (Fig. 5b inset). Considering the growth delay, it was possible that *Sox10* expression had simply not been induced yet in the posterior trunk region of the mutant embryo at E9.5. However, by E10.5, we still detected no

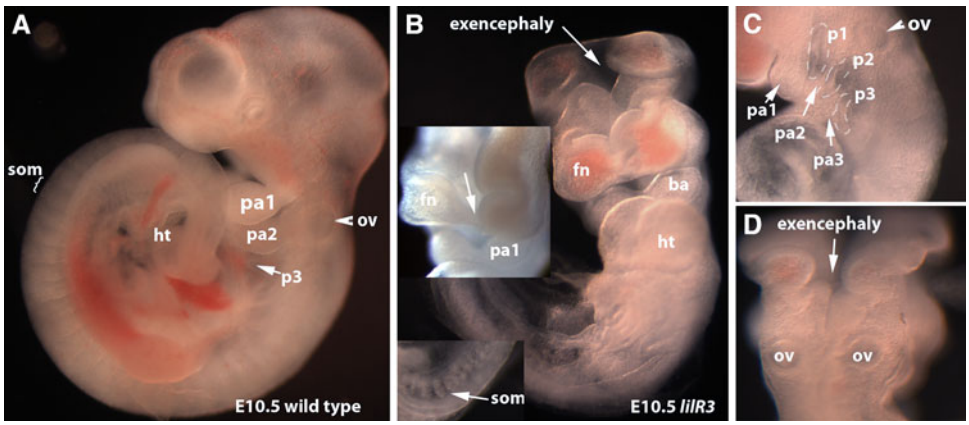

Fig. 4 Morphological defects of the E10.5 homozygous $Opa1^{lilR3}$ mutant embryo. Wild-type littermate control (**a**) and homozygous $Opa1^{lilR3}$ (**b-d**) embryos at E10.5. **a** Lateral view of a littermate control. **b** Ventral view of $Opa1^{lilR3}$ mutant. Inset is a higher-magnification view of the hypomorphic somites. **c** Lateral view of the craniofacial and pharyngeal structures. Note the blood pooling in the frontonasal process, cranial folds, and the pharyngeal arches. **d** Dorsal view of exencephaly. *pa* pharyngeal arches, *fn* frontonasal process, *som* somites, *ht* heart tube, *ba* branchial arch, *ov* otic vesicles. Anterior is up, posterior is down

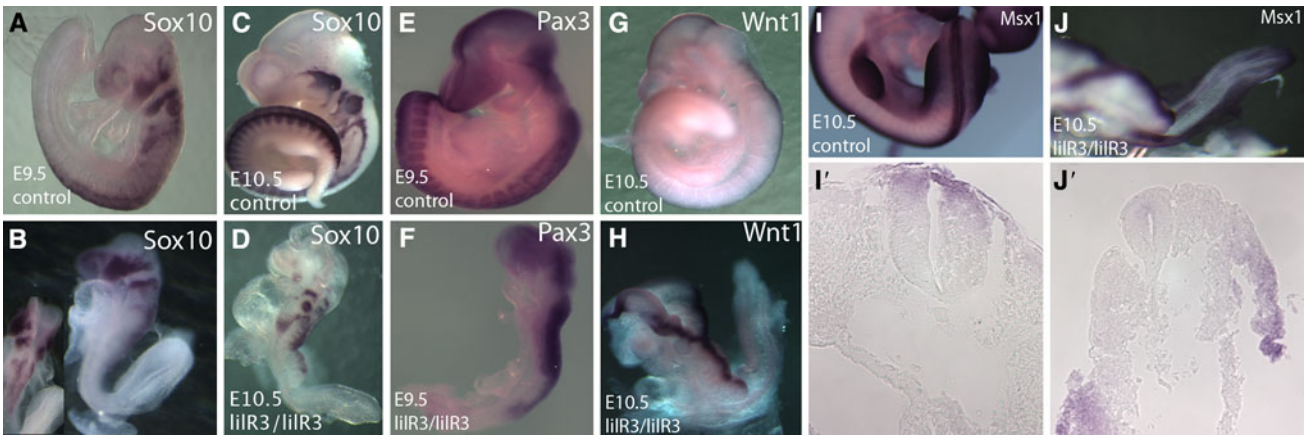

Fig. 5 Misexpression of key genes involved in neural crest development. Whole-mount in situ hybridization of **a**, **c**, **e**, **g**, **i**, **i′** wild-type control littermates and **b**, **d**, **f**, **h**, **j**, **j′** $Opa1^{lilR3}$ homozygous mutant embryos. Expression of a neural crest marker *Sox10* at E9.5 in **a** control and **b** $Opa1^{lilR3}$ embryos and in E10.5 **c** control and **d** $Opa1^{lilR3}$ embryos. *Pax3* expression in E9.5 **e** control and **f** $Opa1^{lilR3}$ embryos. Expression of *Wnt1* in E10.5 **g** control and **h** $Opa1^{lilR3}$ mutant embryos. *Msx1* expression at E10.5 in **i** control and **j** $Opa1^{lilR3}$ mutant embryos

Sox10 expression in the posterior trunk of the $Opa1^{lilR3}$ mutant, whereas there was robust *Sox10* expression along the entire length of the A-P axis in the control (Fig. 5c, d). Furthermore, we found that *Sox10* expression was diminished in the craniofacial tissues of the $Opa1^{lilR3}$ mutant at E10.5.

Pax3, *Wnt1*, and *Msx1* are all expressed in the neural tube and are instrumental in neural closure and neural crest development. We examined *Pax3* expression at E9.5 and found relatively normal expression in the head, anterior neural tube, and lateral mesoderm of the $Opa1^{lilR3}$ mutant embryos, but no expression in the somites (Fig. 5e, f). However, analogous to the axial difference we saw in *Sox10* expression, *Pax3* expression was absent in the posterior of $Opa1^{lilR3}$ embryos. We found this same pattern with expression of both *Wnt1* and *Msx1* at E10.5, when both are missing in the posterior (Fig. 5g–j).

Anterior-posterior patterning of the axis is grossly normal in the $Opa1^{lilR3}$ mutant

An interesting aspect of the expression analysis above is that *Sox10*, *Wnt1*, *Pax3*, and *Msx1* were most severely disrupted in the posterior of the $Opa1^{lilR3}$ mutant embryos. It is unclear why particular subsets of genes are not expressed in specific cell types or at certain axial positions, while others appear normal. Axial-specific defects could be explained if A–P patterning of the embryonic body plan was disrupted by the $Opa1^{lilR3}$ mutation. Since *Hox* genes regulate the establishment of the A–P axis, we examined the expression of *Hoxb6* and *Hoxb9* and found they were normal (Fig. 6). Thus, at a gross level, the initial A-P patterning is not disrupted in the $Opa1^{lilR3}$ mutants.

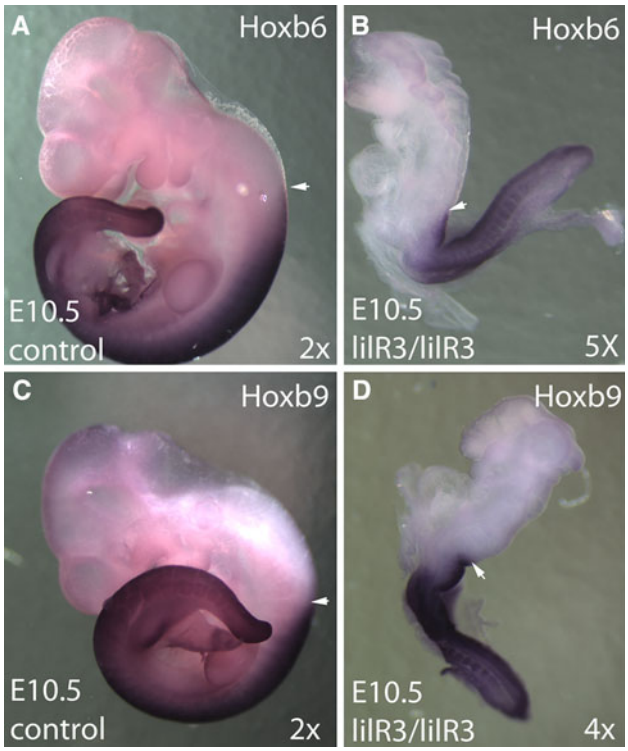

Fig. 6 Expression of *Hoxb6* and *Hoxb9* appears grossly normal in the $Opa1^{lilR3}$ mutant embryo. Whole-mount in situ hybridization of E10.5 (**a**, **c**) control littermates and (**b**, **d**) $Opa1^{lilR3}$ mutants. *Arrows* indicate anterior limits of expression

Somitic expression of proliferative genes is diminished or lost, explaining the failure in somite development

The somites in $Opa1^{lilR3}$ embryos formed but looked abnormal; so, in addition to *Pax3* we investigated somitic development by examining *Pax1* and *Pax9* expression.

Pax1 and *Pax9* are paired box transcription factors expressed in the sclerotome, the ventromedial region of the somites. Consistent with the morphological defects we observed in somites, we found that like *Pax3* expression, expression of *Pax1* and *Pax9* was diminished or lost in all somites of the *Opa1*^{lilR3} mutants (Fig. 5f). The absence of *Pax1*, *3*, and *9* indicated that the somites do not follow their normal developmental program in *Opa1*^{lilR3} mutants (Fig. 7a–d), and unlike what we observed with *Wnt1* and *Msx1* expression, *Pax* expression in the somites was disrupted regardless of axial position.

Cell death analysis of *Opa1*^{lilR3} mutant embryos

Several factors prompted us to examine cell death in the *Opa1*^{lilR3} mutants. First, mitochondrial dynamics have been linked to apoptosis. The loss of Opa1 has been found to correlate with increased apoptosis under certain cell culture conditions (Cipolat et al. 2006; Frezza et al. 2006; Olichon et al. 2007). Second, *Pax3* homozygous mutants display increased apoptosis in somites and the neural tube (Goulding et al. 1991). Third, the loss of *Pax1* and *Pax9* results in more apoptosis in the sclerotome (Peters et al. 1999). Finally, the lack of *Sox10*, *Wnt1*, *Pax3*, and *Msx1* expression in the posterior of *Opa1*^{lilR3} embryos could have been explained by the death of those cells. Thus, we analyzed cell death using LysoTracker Red, a vital dye that monitors phagolysosomal activity during the engulfment of apoptotic bodies (Zucker et al. 1999). LysoTracker Red has the advantage of permeating whole embryos well, enabling us to visualize cell death throughout the embryo.

At E9.5 we found that the pattern of cell death was relatively similar in the E9.5 *Opa1*^{lilR3} mutant and the wild-type control embryos, indicating that the aberrant gene expression we observe between *Opa1*^{lilR3} mutant and wild-type littermates is not simply a consequence of general cell death (Fig. 8a, b). By E10.5 we observed an expansion in the pattern of cell death in *Opa1*^{lilR3} mutant embryos compared with wild-type (Fig. 8c, d). From dorsal views, it was apparent that the cell death was concentrated in the

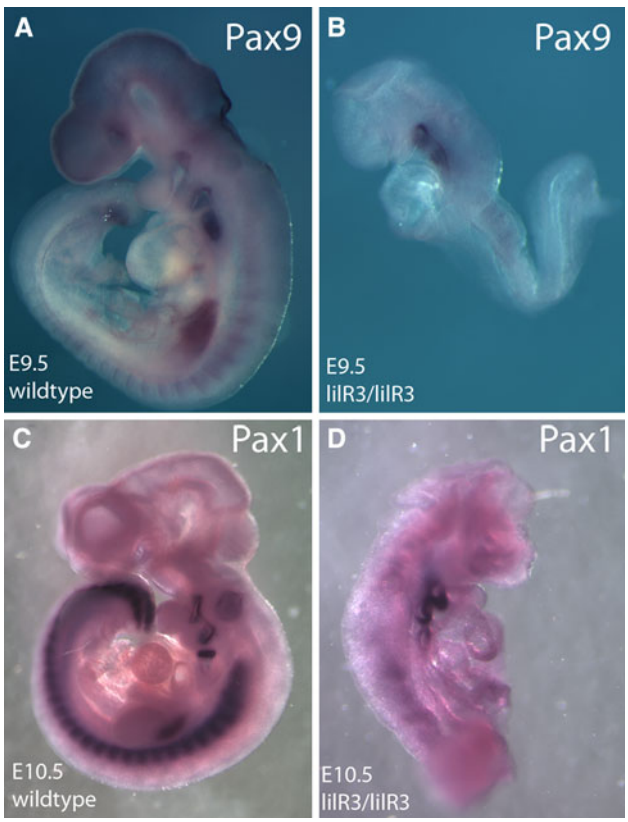

Fig. 7 Hypomorphic somite development is likely due to a failure to express *Pax1* and *Pax9*. *Pax9* expression in E9.5 **a** control and **b** *Opa1*^{lilR3} embryos. *Pax1* expression at E10.5 in **c** control and **d** *Opa1*^{lilR3} mutant embryos. Note that *Pax9* and *Pax1* are expressed in the pharyngeal endoderm but not in the somites of the *Opa1*^{lilR3} mutant compared with the control littermates. Both genes are required for somite growth

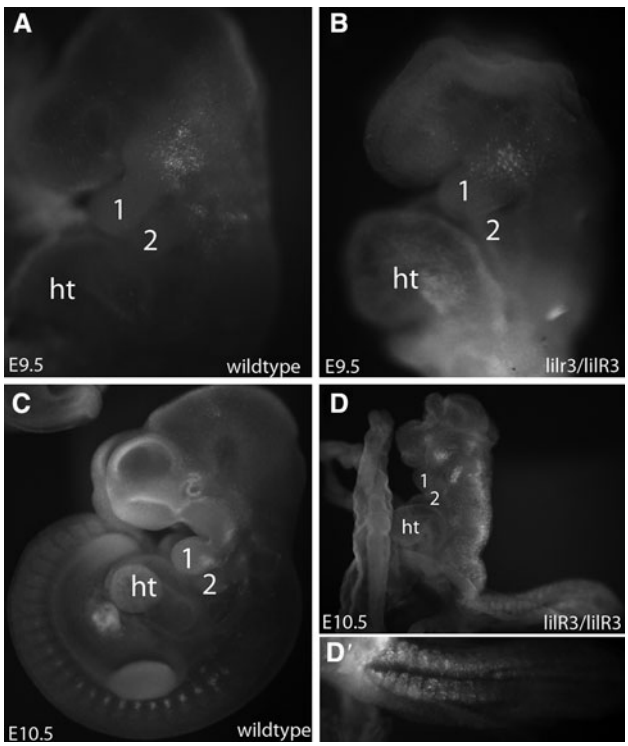

Fig. 8 Cell death is not responsible for the growth delay in the *lilR3* homozygous mutant embryos. Cell death as assessed in whole embryos using LysoTracker. The pattern of cell death is comparable to that seen in **a** control and **b** *Opa1*^{lilR3} mutant embryos at E9.5. A more broad pattern of cell death is visible in both **c** control and **d** *Opa1*^{lilR3} embryos at E10.5. **d′** A higher-magnification view of cell death in the somites of the *Opa1*^{lilR3} mutant embryo in (**d**). However, cell death is visible along the neuraxis of the mutant and not in the control. 1 and 2, arches 1 and 2; ht, heart

somites, consistent with the absence of *Pax1*, *3*, or *9* expression in somites along the A-P axis.

Discussion

Here we characterize a novel allele of *Opa1* and for the first time ascribe a function to the middle domain of the Opa1 protein. Based on our observation of the mitochondrial fragmentation phenotype in *lilR3* MEFs and the mislocalization of Opa1 protein in the embryos, we are confident that the A → G transition in *Opa1* is responsible for the *lilR3* phenotype. Mitochondrial fragmentation in the MEFs was similar to mitochondrial fragmentation in cell lines from patients with heterozygous mutations in *Opa1* as well as cell lines in which Opa1 expression was knocked down by siRNA (Amati-Bonneau et al. 2005, 2008, 2009; Chen et al. 2005; Cipolat et al. 2004; Griparic et al. 2004; Olichon et al. 2003, 2007; Zanna et al. 2008). Three ADOA patients have been identified whose mutations disrupt W616 as the *lilR3* allele does (Alexander et al. 2000; Ferre et al. 2009). Furthermore, the embryos die at midgestation, which is about the same time as embryos with mutations in either one of the other components of the fusion machinery (Mfn1 and Mfn2) or the proteins that process Opa1 (Phb2) (Chen et al. 2003; Merkwirth et al. 2008; Park et al. 2005). Thus our data are consistent with Opa1 function being dependent on its mitochondrial localization.

The mislocalization of Opa1 protein in the *lilR3* mutant raised the possibility that gain of function due to the accumulation of Opa1 in the cytosol contributes to the phenotype. While this remains a possibility, it seems unlikely given the previous analysis of two distinct ENU-induced point mutations in *Opa1* (Alavi et al. 2007; Davies et al. 2007). In both cases, the authors found a decrease in Opa1 protein expression in the heterozygous mutants. One group analyzed the cytosolic and mitochondrial cell fractions of their ENU allele and saw no mislocalization of Opa1 protein (Alavi et al. 2007). Thus, these two alleles appear to result in less Opa1 protein. Both groups focused their work on careful characterization of the heterozygous mice as animal models for ADOA; however, they did report that homozygous embryos died around E11.5, and in one case published a photo of the mutant embryo that displayed features similar to those we observed (Davies et al. 2007). Specifically, their photograph showed an embryo with growth delay, exencephaly, and a body shape that is characteristic of the *lilR3* phenotype. While their analysis was on a distinct genetic background, the identical times of death in all three alleles, the overlapping phenotypes, and the suggestion that the other two alleles result in the loss of Opa1 protein are most consistent with the *lilR3* mutation being a loss-of-function allele. Although technically it is possible that one of the 13 remaining genes in the *lilR3* interval is also affected, the facts that the distinct *Opa1* alleles phenocopy one another and were discovered independently along with the mislocalization of Opa1 protein in *lilR3* embryos are most consistent with *lilR3* affecting Opa1 alone.

The precise defect underlying the lethality of $Opa1^{lilR3}$ mutants remains unclear. Mitochondrial dysfunction in humans has been linked to a variety of cardiomyopathies, and other mouse mutants with defects in mitochondrial fission and fusion display abnormal cardiac function, so it is possible that $Opa1^{lilR3}$ lethality may be due to abnormal heart development (Marin-Garcia et al. 1995, 1996, 2001; Zell et al. 1997).

Our analysis provides the first molecular characterization of the homozygous phenotype involving loss of Opa1 function. Curiously, we saw that gene expression was more affected posteriorly despite a normal anterior-posterior axis. The phenotype we observed raises the possibility that distinct types of neural crest may have distinct requirements for Opa1, or even for mitochondrial dynamics in general. Ever since the discovery linking Opa1 to ADOA, it has been clear that retinal ganglion cells are more sensitive to decreased Opa1 than other cells (Alexander et al. 2000; Delettre et al. 2000). Several factors are proposed to explain these differences. First, retinal ganglion cells may preferentially express certain Opa1 isoforms. Second, cells have distinct energy needs, and the speculation is that those with the highest needs would be most sensitive to perturbations in mitochondrial dynamics. Furthermore, while mitochondria are most famous for ATP production, they also function to buffer intracellular calcium and are central to apoptosis. Thus, the loss of Opa1 and the resulting change in mitochondrial shape could influence any of these processes.

A reasonable interpretation of the distinct patterns of cell death and gene expression we saw in $Opa1^{lilR3}$ embryos is that these patterns correlate to the relative importance of these distinct mitochondrial processes in different cell populations at specific times in development. Our analysis points to tissue-specific functions of Opa1. The somites give rise to the skeleton and muscle of the adult. Several ADOA patients have been reported to have additional phenotypes, including myopathy, deafness, and ataxia (Chen et al. 2007; Ferraris et al. 2008; Stewart et al. 2008; Treft et al. 1984). Other human conditions associated with mitochondrial dysfunction display abnormal processing of Opa1 and skeletal defects (Duvezin-Caubet et al. 2006). The somite-specific cell death we see in our $Opa1^{lilR3}$ mutants would be consistent with somatic lineage being sensitive to the loss of the apoptotic role of Opa1.

In sum, the $Opa1^{lilR3}$ mutant mouse provides an excellent in vivo model for exploring the cell-specific roles of

Opa1. While it remains unclear if any of the identified *Opa1* alleles are null alleles, the *Opa1*^{lilR3} allele permits investigation of Opa1 function that depends on its localization to mitochondria. Our data suggest that tissues not typically believed to be affected in ADOA patients could be involved in the disease. There are at least ten mitochondrial proteins implicated in neurogenerative diseases such as Charcot-Marie-Toothe, hereditary spastic paraplegia, Friedrich's ataxia, and familial Parkinson's. Defining the mammalian loss-of-function roles of specific Opa1 isoforms could reveal fundamental mechanisms shared by these disorders.

Experimental procedures

Mutant phenotypic and genotypic identification

The *lilR3* mutation was generated by ENU mutagenesis as described previously and analyzed in C3H/HeJ mice (Garcia-Garcia et al. 2005; Kasarskis et al. 1998). Genetic mapping of *Opa1*^{lilR3} was performed by linkage analysis of 2,876 opportunities for recombination with SSLP markers (www.informatics.jax.org and http://mouse.ski.mskcc.org). We obtained physical map information from Ensembl (http://www.ensembl.org/Mus_musculus/index.html).

cDNAs of four genes in the *lilR3* interval (*Opa1*, *Hes1*, *ApoD*, and *Lrrc15*) were amplified by RT-PCR (Superscript One-Step RT-PCR, Invitrogen, Carlsbad, CA) using RNA from E10.5 *lilR3* embryos. DNAs from the corresponding genomic regions were also amplified. All amplicons were sequenced and, when compared with the C57BL/6 reference sequence (http://www.ensembl.org/Mus_musculus/index.html), an A-to-T mutation was found in intron 19 of *Opa1*. Subsequent analysis of C57/B6 DNA has verified this mutation. We found no mutations in any of the other sequenced genes in the interval.

Western blotting

E10.5 *Opa1*^{lilR3} embryos were homogenized to obtain the crude mitochondrial fraction as described in Alavi et al. (2007). The total protein concentration was determined through Bradford assay (Bio-Rad, Hercules, CA) following the manufacturer's recommendations. Equal amounts of total protein were loaded on a gradient 4-20% SDS-PAGE gel (Bio-Rad) and transferred onto a nitrocellulose membrane (Amersham Bioscience, Piscataway, NJ). The membrane was subjected to Western blot analysis with antibodies against Opa1 (BD Pharmingen, Franklin Lakes, NJ), α-tubulin (Sigma, St. Louis, MO), and cytochrome *c* (BD Pharmingen), followed by immunodetection using an ECL chemiluminescence system (GE Healthcare Biosciences, Piscataway, NJ).

MitoTracker assay

Opa1^{lilR3}/*Opa1*^{lilR3}, *Opa1*^{lilR3}/+, and wild-type MEFs were grown on coverslips and treated with MitoTracker Red CM-H2XRos (Invitrogen, M-7513) in DMEM (high glucose, 10% FBS, penicillin/streptomycin) at a final concentration of 250 nM for 45 min at 37°C, 5% CO_2. After treatment, cells were washed in DMEM (high glucose, 10% FBS, penicillin/streptomycin) for 1 h at 37°C, 5% CO_2. The coverslips were then fixed for 10 min in 4% paraformaldehyde at room temperature, rinsed in PBS for 5 min, and mounted in ProLong Gold antifade reagent (Invitrogen, P36934). Images were captured using the Zeiss LSM 510 META confocal at 63× with and without optical zoom.

Analysis of mutant phenotype

Embryos were dissected in PBS containing 0.4% BSA at different stages as assessed by the presence of vaginal plugs in mothers. Whole-mount RNA in situ hybridization activity was performed as described (Belo et al. 1997; Schaeren-Wiemers and Gerfin-Moser 1993). Probes for *Sox10*, *Pax3*, *Pax1*, *Pax9*, *HoxB5*, *HoxB6*, *Wnt1*, and *Msx1* have been previously reported (Becker et al. 1996; Chalepakis et al. 1991; Goulding et al. 1991; Hakami et al. 2006; Krumlauf et al. 1987; Parr et al. 1993; Peters et al. 1995).

Analysis of cell death

To analyze cell death, freshly dissected embryos were washed two times for 5 min in 1× PBS/0.1% Triton X-100 at room temperature, then incubated in 1× PBS/0.1% Triton X-100 containing 50 nM LysoTracker Red (Invitrogen) for 30 min at room temperature. Embryos could be visualized immediately or fixed in 4% paraformaldehyde overnight at 4°C. The embryos were rinsed in 1× PBS, and labeled cells were visualized with a Leica MZFLIII microscope under UV light using a GFP filter. Images were captured using a Q-imaging Retiga EXi camera.

Acknowledgments We are grateful to Michael Wyler and Kathryn Anderson for the initial identification of the *lilR3* phenotype in the course of the Sloan-Kettering Mouse Mutagenesis Project. Cheryl Strauss, Laura Mariani, Vanessa Horner, and Chen-Ying Su provided valuable comments on the manuscript. This work was funded by a Hitchings-Elion Career Development Award from the Burroughs Wellcome Fund and a Muscular Dystrophy Development Grant, as well as by Emory University Development Funds. The *Opa1*^{lilR3} allele has been submitted to the Mouse Genome Informatics (MGI) database.

References

Alavi MV, Bette S, Schimpf S, Schuettauf F, Schraermeyer U, Wehrl HF, Ruttiger L, Beck SC, Tonagel F, Pichler BJ, Knipper M, Peters T, Laufs J, Wissinger B (2007) A splice site mutation in the murine *Opa1* gene features pathology of autosomal dominant optic atrophy. Brain 130:1029–1042

Alexander C, Votruba M, Pesch UE, Thiselton DL, Mayer S, Moore A, Rodriguez M, Kellner U, Leo-Kottler B, Auburger G, Bhattacharya SS, Wissinger B (2000) OPA1, encoding a dynamin-related GTPase, is mutated in autosomal dominant optic atrophy linked to chromosome 3q28. Nat Genet 26:211–215

Amati-Bonneau P, Guichet A, Olichon A, Chevrollier A, Viala F, Miot S, Ayuso C, Odent S, Arrouet C, Verny C, Calmels MN, Simard G, Belenguer P, Wang J, Puel JL, Hamel C, Malthiery Y, Bonneau D, Lenaers G, Reynier P (2005) OPA1 R445H mutation in optic atrophy associated with sensorineural deafness. Ann Neurol 58:958–963

Amati-Bonneau P, Valentino ML, Reynier P, Gallardo ME, Bornstein B, Boissiere A, Campos Y, Rivera H, de la de la Aleja JG, Carroccia R, Lommarini L, Labauge P, Figarella-Branger D, Marcorelles P, Furby A, Beauvais K, Letournel F, Liguori R, La Morgia C, Montagna P, Liguori M, Zanna C, Rugolo M, Cossarizza A, Wissinger B, Verny C, Schwarzenbacher R, Martin MA, Arenas J, Ayuso C, Garesse R, Lenaers G, Bonneau D, Carelli V (2008) *OPA1* mutations induce mitochondrial DNA instability and optic atrophy 'plus' phenotypes. Brain 131:338–351

Amati-Bonneau P, Milea D, Bonneau D, Chevrollier A, Ferre M, Guillet V, Gueguen N, Loiseau D, de Crescenzo MA, Verny C, Procaccio V, Lenaers G, Reynier P (2009) OPA1-associated disorders: phenotypes and pathophysiology. Int J Biochem Cell Biol 41:1855–1865

Becker D, Eid R, Schughart K (1996) The limb/LPM enhancer of the murine *Hoxb6* gene: reporter gene analysis in transgenic embryos and studies of DNA-protein interactions. Pharm Acta Helv 71:29–35

Belo JA, Bouwmeester T, Leyns L, Kertesz N, Gallo M, Follettie M, De Robertis EM (1997) Cerberus-like is a secreted factor with neutralizing activity expressed in the anterior primitive endoderm of the mouse gastrula. Mech Dev 68:45–57

Bleazard W, McCaffery JM, King EJ, Bale S, Mozdy A, Mozdy A, Nunnari J, Shaw JM (1999) The dynamin-related GTPase Dnm1 regulates mitochondrial fission in yeast. Nat Cell Biol 1:298–304

Chalepakis G, Fritsch R, Fickenscher H, Deutsch U, Goulding M, Gruss P (1991) The molecular basis of the undulated/Pax-1 mutation. Cell 66:873–884

Chen H, Chan DC (2004) Mitochondrial dynamics in mammals. Curr Top Dev Biol 59:119–144

Chen H, Chan DC (2009) Mitochondrial dynamics—fusion, fission, movement, and mitophagy—in neurodegenerative diseases. Hum Mol Genet 18:R169–R176

Chen H, Detmer SA, Ewald AJ, Griffin EE, Fraser SE, Chan DC (2003) Mitofusins Mfn1 and Mfn2 coordinately regulate mitochondrial fusion and are essential for embryonic development. J Cell Biol 160:189–200

Chen H, Chomyn A, Chan DC (2005) Disruption of fusion results in mitochondrial heterogeneity and dysfunction. J Biol Chem 280:26185–26192

Chen S, Zhang Y, Wang Y, Li W, Huang S, Chu X, Wang L, Zhang M, Liu Z (2007) A novel *OPA1* mutation responsible for autosomal dominant optic atrophy with high frequency hearing loss in a Chinese family. Am J Ophthalmol 143:186–188

Cipolat S, Martins de Brito O, Dal Zilio B, Scorrano L (2004) OPA1 requires mitofusin 1 to promote mitochondrial fusion. Proc Natl Acad Sci USA 101:15927–15932

Cipolat S, Rudka T, Hartmann D, Costa V, Serneels L, Craessaerts K, Metzger K, Frezza C, Annaert W, D'Adamio L, Derks C, Dejaegere T, Pellegrini L, D'Hooge L, Scorrano L, De Strooper B (2006) Mitochondrial rhomboid PARL regulates cytochrome c release during apoptosis via OPA1-dependent cristae remodeling. Cell 126:163–175

Davies VJ, Hollins AJ, Piechota MJ, Yip W, Davies JR, White KE, Nicols PP, Boulton ME, Votruba M (2007) Opa1 deficiency in a mouse model of autosomal dominant optic atrophy impairs mitochondrial morphology, optic nerve structure and visual function. Hum Mol Genet 16:1307–1318

Delettre C, Lenaers G, Griffoin JM, Gigarel N, Lorenzo C, Belenguer P, Pelloquin L, Grosgeorge J, Turc-Carel C, Perret E, Astarie-Dequeker C, Lasquellec L, Arnaud B, Ducommun B, Kaplan J, Hamel CP (2000) Nuclear gene *OPA1*, encoding a mitochondrial dynamin-related protein, is mutated in dominant optic atrophy. Nat Genet 26:207–210

Delettre C, Griffoin JM, Kaplan J, Dollfus H, Lorenz B, Faivre L, Lenaers G, Belenguer P, Hamel CP (2001) Mutation spectrum and splicing variants in the *OPA1* gene. Hum Genet 109:584–591

Detmer SA, Chan DC (2007) Functions and dysfunctions of mitochondrial dynamics. Nat Rev Mol Cell Biol 8:870–879

Duchen MR (2000) Mitochondria and calcium: from cell signalling to cell death. J Physiol 529(Pt 1):57–68

Duvezin-Caubet S, Jagasia R, Wagener J, Hofmann S, Trifunovic A, Hansson A, Chomyn A, Bauer MF, Attardi G, Larsson NG, Neupert W, Reichert AS (2006) Proteolytic processing of OPA1 links mitochondrial dysfunction to alterations in mitochondrial morphology. J Biol Chem 281:37972–37979

Fekkes P, Shepard KA, Yaffe MP (2000) Gag3p, an outer membrane protein required for fission of mitochondrial tubules. J Cell Biol 151:333–340

Ferraris S, Clark S, Garelli E, Davidzon G, Moore SA, Kardon RH, Bienstock RJ, Longley MJ, Mancuso M, Gutierrez Rios P, Hirano M, Copeland WC, DiMauro S (2008) Progressive external ophthalmoplegia and vision and hearing loss in a patient with mutations in POLG2 and OPA1. Arch Neurol 65:125–131

Ferre M, Bonneau D, Milea D, Chevrollier A, Verny C, Dollfus H, Ayuso C, Defoort S, Vignal C, Zanlonghi X, Charlin JF, Kaplan J, Odent S, Hamel CP, Procaccio V, Reynier P, Amati-Bonneau P (2009) Molecular screening of 980 cases of suspected hereditary optic neuropathy with a report on 77 novel *OPA1* mutations. Hum Mutat 30:E692–E705

Frezza C, Cipolat S, Martins de Brito O, Micaroni M, Beznoussenko GV, Rudka T, Bartoli D, Polishuck RS, Danial NN, De Strooper B, Scorrano L (2006) OPA1 controls apoptotic cristae remodeling independently from mitochondrial fusion. Cell 126:177–189

Garcia-Garcia MJ, Eggenschwiler JT, Caspary T, Alcorn HL, Wyler MR, Huangfu D, Rakeman AS, Lee JD, Feinberg EH, Timmer JR, Anderson KV (2005) Analysis of mouse embryonic patterning and morphogenesis by forward genetics. Proc Natl Acad Sci USA 102:5913–5919

Goulding MD, Chalepakis G, Deutsch U, Erselius JR, Gruss P (1991) Pax-3, a novel murine DNA binding protein expressed during early neurogenesis. EMBO J 10:1135–1147

Griparic L, van der Wel NN, Orozco IJ, Peters PJ, van der Bliek AM (2004) Loss of the intermembrane space protein Mgm1/OPA1 induces swelling and localized constrictions along the lengths of mitochondria. J Biol Chem 279:18792–18798

Griparic L, Kanazawa T, van der Bliek AM (2007) Regulation of the mitochondrial dynamin-like protein Opa1 by proteolytic cleavage. J Cell Biol 178:757–764

Hakami RM, Hou L, Baxter LL, Loftus SK, Southard-Smith EM, Incao A, Cheng J, Pavan WJ (2006) Genetic evidence does not support direct regulation of EDNRB by SOX10 in migratory neural crest and the melanocyte lineage. Mech Dev 123:124–134

Hales KG, Fuller MT (1997) Developmentally regulated mitochondrial fusion mediated by a conserved, novel, predicted GTPase. Cell 90:121–129

Herlan M, Vogel F, Bornhovd C, Neupert W, Reichert AS (2003) Processing of Mgm1 by the rhomboid-type protease Pcp1 is required for maintenance of mitochondrial morphology and of mitochondrial DNA. J Biol Chem 278:27781–27788

Hermann GJ, Thatcher JW, Mills JP, Hales KG, Fuller MT, Nunnari J, Shaw JM (1998) Mitochondrial fusion in yeast requires the transmembrane GTPase Fzo1p. J Cell Biol 143:359–373

James DI, Parone PA, Mattenberger Y, Martinou JC (2003) hFis1, a novel component of the mammalian mitochondrial fission machinery. J Biol Chem 278:36373–36379

Kasarskis A, Manova K, Anderson KV (1998) A phenotype-based screen for embryonic lethal mutations in the mouse. Proc Natl Acad Sci USA 95(13):7485–7490

Kim J, Lo L, Dormand E, Anderson DJ (2003) SOX10 maintains multipotency and inhibits neuronal differentiation of neural crest stem cells. Neuron 38:17–31

Kivlin JD, Lovrien EW, Bishop DT, Maumenee IH (1983) Linkage analysis in dominant optic atrophy. Am J Hum Genet 35:1190–1195

Kjer B, Eiberg H, Kjer P, Rosenberg T (1996) Dominant optic atrophy mapped to chromosome 3q region. II. Clinical and epidemiological aspects. Acta Ophthalmol Scand 74:3–7

Knott AB, Perkins G, Schwarzenbacher R, Bossy-Wetzel E (2008) Mitochondrial fragmentation in neurodegeneration. Nat Rev Neurosci 9:505–518

Kroemer G, Reed JC (2000) Mitochondrial control of cell death. Nat Med 6:513–519

Krumlauf R, Holland PW, McVey JH, Hogan BL (1987) Developmental and spatial patterns of expression of the mouse homeobox gene, *Hox2.1*. Development 99:603–617

Labrousse AM, Zappaterra MD, Rube DA, van der Bliek AM (1999) *C. elegans* dynamin-related protein DRP-1 controls severing of the mitochondrial outer membrane. Mol Cell 4:815–826

Lee YJ, Jeong SY, Karbowski M, Smith CL, Youle RJ (2004) Roles of the mammalian mitochondrial fission and fusion mediators Fis1, Drp1, and Opa1 in apoptosis. Mol Biol Cell 15:5001–5011

Marin-Garcia J, Goldenthal MJ, Pierpont ME, Ananthakrishnan R (1995) Impaired mitochondrial function in idiopathic dilated cardiomyopathy: biochemical and molecular analysis. J Card Fail 1:285–291

Marin-Garcia J, Goldenthal MJ, Ananthakrishnan R, Pierpont ME, Fricker FJ, Lipshultz SE, Perez-Atayde A (1996) Mitochondrial function in children with idiopathic dilated cardiomyopathy. J Inherit Metab Dis 19:309–312

Marin-Garcia J, Goldenthal MJ, Moe GW (2001) Mitochondrial pathology in cardiac failure. Cardiovasc Res 49:17–26

Merkwirth C, Dargazanli S, Tatsuta T, Geimer S, Lower B, Wunderlich FT, von Kleist-Retzow JC, Waisman A, Westermann B, Langer T (2008) Prohibitins control cell proliferation and apoptosis by regulating OPA1-dependent cristae morphogenesis in mitochondria. Genes Dev 22:476–488

Misaka T, Miyashita T, Kubo Y (2002) Primary structure of a dynamin-related mouse mitochondrial GTPase and its distribution in brain, subcellular localization, and effect on mitochondrial morphology. J Biol Chem 277:15834–15842

Mozdy AD, McCaffery JM, Shaw JM (2000) Dnm1p GTPase-mediated mitochondrial fission is a multi-step process requiring the novel integral membrane component Fis1p. J Cell Biol 151:367–380

Olichon A, Baricault L, Gas N, Guillou E, Valette A, Belenguer P, Lenaers G (2003) Loss of OPA1 perturbates the mitochondrial inner membrane structure and integrity, leading to cytochrome c release and apoptosis. J Biol Chem 278:7743–7746

Olichon A, Landes T, Arnaune-Pelloquin L, Emorine LJ, Mils V, Guichet A, Delettre C, Hamel C, Amati-Bonneau P, Bonneau D, Reynier P, Lenaers G, Belenguer P (2007) Effects of OPA1 mutations on mitochondrial morphology and apoptosis: relevance to ADOA pathogenesis. J Cell Physiol 211:423–430

Park SE, Xu J, Frolova A, Liao L, O'Malley BW, Katzenellenbogen BS (2005) Genetic deletion of the repressor of estrogen receptor activity (REA) enhances the response to estrogen in target tissues in vivo. Mol Cell Biol 25:1989–1999

Parr BA, Shea MJ, Vassileva G, McMahon AP (1993) Mouse *Wnt* genes exhibit discrete domains of expression in the early embryonic CNS and limb buds. Development 119:247–261

Peters H, Doll U, Niessing J (1995) Differential expression of the chicken *Pax-1* and *Pax-9* gene: in situ hybridization and immunohistochemical analysis. Dev Dyn 203:1–16

Peters H, Wilm B, Sakai N, Imai K, Maas R, Balling R (1999) Pax1 and Pax9 synergistically regulate vertebral column development. Development 126:5399–5408

Rapaport D, Brunner M, Neupert W, Westermann B (1998) Fzo1p is a mitochondrial outer membrane protein essential for the biogenesis of functional mitochondria in *Saccharomyces cerevisiae*. J Biol Chem 273:20150–20155

Rizzuto R, Bernardi P, Pozzan T (2000) Mitochondria as all-round players of the calcium game. J Physiol 529(Pt 1):37–47

Rochais F, Dandonneau M, Mesbah K, Jarry T, Mattei MG, Kelly RG (2009) Hes1 is expressed in the second heart field and is required for outflow tract development. PLoS One 4:e6267

Schaeren-Wiemers N, Gerfin-Moser A (1993) A single protocol to detect transcripts of various types and expression levels in neural tissue and cultured cells: in situ hybridization using digoxigenin-labelled cRNA probes. Histochemistry 100:431–440

Smirnova E, Griparic L, Shurland DL, van der Bliek AM (2001) Dynamin-related protein Drp1 is required for mitochondrial division in mammalian cells. Mol Biol Cell 12:2245–2256

Song Z, Chen H, Fiket M, Alexander C, Chan DC (2007) OPA1 processing controls mitochondrial fusion and is regulated by mRNA splicing, membrane potential, and Yme1L. J Cell Biol 178:749–755

Spinazzi M, Cazzola S, Bortolozzi M, Baracca A, Loro E, Casarin A, Solaini G, Sgarbi G, Casalena G, Cenacchi G, Malena A, Frezza C, Carrara F, Angelini C, Scorrano L, Salviati L, Vergani L (2008) A novel deletion in the GTPase domain of OPA1 causes defects in mitochondrial morphology and distribution, but not in function. Hum Mol Genet 17:3291–3302

Stewart JD, Hudson G, Yu-Wai-Man P, Blakeley EL, He L, Horvath R, Maddison P, Wright A, Griffiths PG, Turnbull DM, Taylor RW, Chinnery PF (2008) OPA1 in multiple mitochondrial DNA deletion disorders. Neurology 71:1829–1831

Tieu Q, Nunnari J (2000) Mdv1p is a WD repeat protein that interacts with the dynamin-related GTPase, Dnm1p, to trigger mitochondrial division. J Cell Biol 151:353–366

Treft RL, Sanborn GE, Carey J, Swartz M, Crisp D, Wester DC, Creel D (1984) Dominant optic atrophy, deafness, ptosis, ophthalmoplegia, dystaxia, and myopathy. A new syndrome. Ophthalmology 91:908–915

Yoon Y, Krueger EW, Oswald BJ, McNiven MA (2003) The mitochondrial protein hFis1 regulates mitochondrial fission in mammalian cells through an interaction with the dynamin-like protein DLP1. Mol Cell Biol 23:5409–5420

Zanna C, Ghelli A, Porcelli AM, Karbowski M, Youle RJ, Schimpf S, Wissinger B, Pinti M, Cossarizza A, Vidoni S, Valentino ML, Rugolo M, Carelli V (2008) OPA1 mutations associated with

dominant optic atrophy impair oxidative phosphorylation and mitochondrial fusion. Brain 131:352–367

Zell R, Geck P, Werdan K, Boekstegers P (1997) TNF-alpha and IL-1 alpha inhibit both pyruvate dehydrogenase activity and mitochondrial function in cardiomyocytes: evidence for primary impairment of mitochondrial function. Mol Cell Biochem 177:61–67

Zucker RM, Hunter ES 3rd, Rogers JM (1999) Apoptosis and morphology in mouse embryos by confocal laser scanning microscopy. Methods 18:473–480